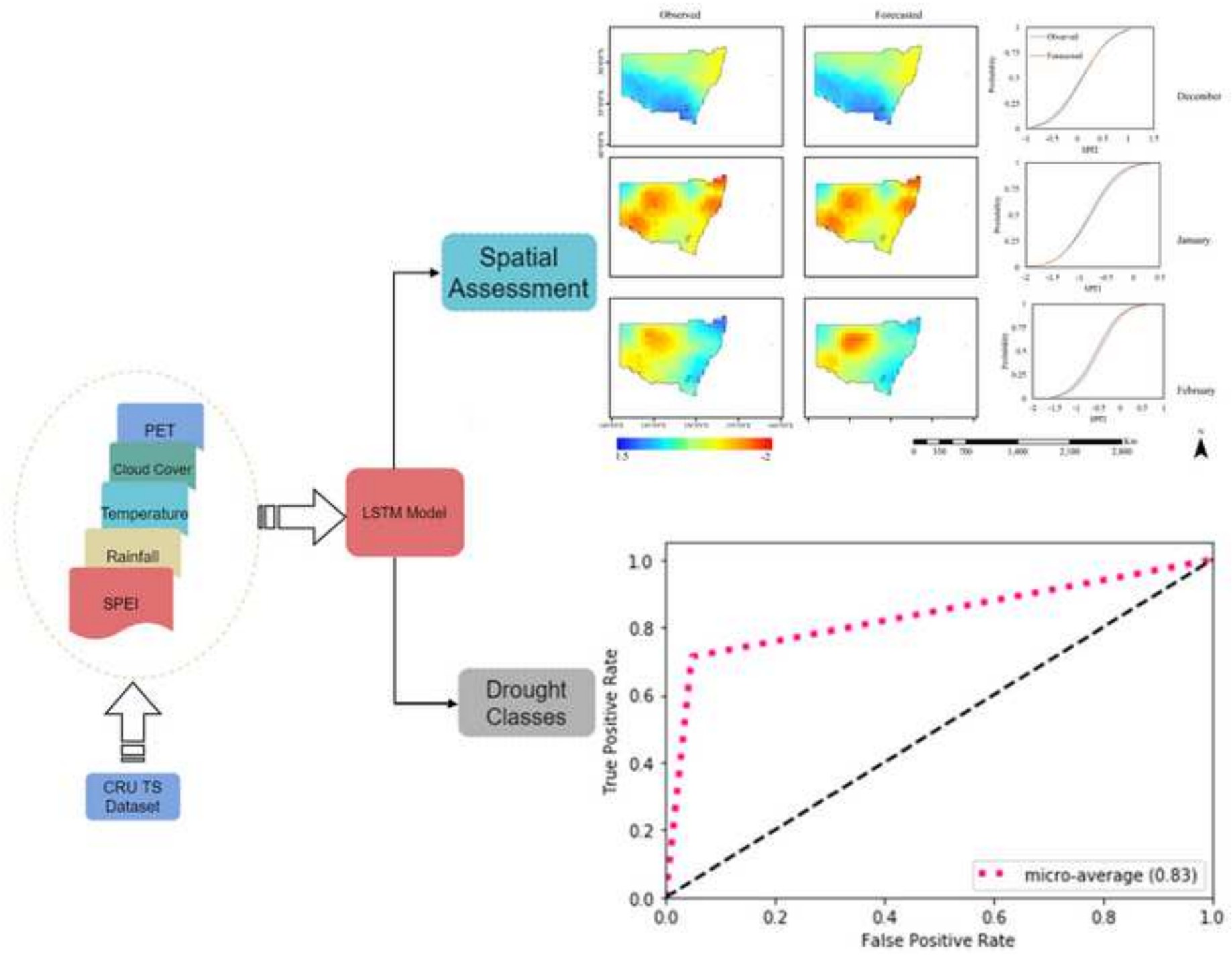


# Journal of Environmental Management

## An Improved SPEI Drought Forecasting Approach using the Long Short-Term Memory Neural Network --Manuscript Draft--

<b>Manuscript Number:</b>	JEMA-D-20-06490R1
<b>Article Type:</b>	Research Article
<b>Keywords:</b>	Standard Precipitation Evaporation Index; New South Wales; Drought Forecasting; Deep Learning
<b>Corresponding Author:</b>	Biswajeet Pradhan, PhD University of Technology Sydney Sydney, AUSTRALIA
<b>First Author:</b>	Abhirup Dikshit, PhD
<b>Order of Authors:</b>	Abhirup Dikshit, PhD Biswajeet Pradhan, PhD Alfredo Huete, PhD
<b>Abstract:</b>	<p>Droughts are slow-moving natural hazards that gradually spread over large areas and capable of extending to continental scales, leading to severe socio-economic damage. A key challenge is developing accurate drought forecast model and understanding a models' capability to examine different drought characteristics. Traditionally, forecasting techniques have used various time-series approaches and machine learning models. However, the use of deep learning methods have not been tested extensively despite its potential to improve our understanding of drought characteristics. The present study uses a deep learning approach, specifically the Long Short-Term Memory (LSTM) to predict a commonly used drought measure, the Standard Precipitation Evaporation Index (SPEI) at two different time scales (SPEI 1, SPEI 3). The model was compared with other common machine learning method, Random Forests, Artificial Neural Networks and applied over the New South Wales (NSW) region of Australia, using hydro-meteorological variables as predictors. The drought index and predictor data were collected from the Climatic Research Unit (CRU) dataset spanning from 1901-2018. We analysed the LSTM forecasted results in terms of several drought characteristics (drought intensity, drought category, or spatial variation) to better understand how drought forecasting was improved. Evaluation of the drought intensity forecasting capabilities of the model were based on three different statistical metrics, Coefficient of Determination (R<sup>2</sup>), Root Mean Square Error (RMSE), and Mean Absolute Error (MAE). The model achieved R<sup>2</sup> value of more than 0.99 for both SPEI 1 and SPEI 3 cases. The variation in drought category forecasted results were studied using a multi-class Receiver Operating Characteristic based Area under Curves (ROC-AUC) approach. The analysis revealed an AUC value of 0.83 and 0.82 for SPEI 1 and SPEI 3 respectively. The spatial variation between observed and forecasted values were analysed for the summer months of 2016-2018. The findings from the study show an improvement relative to machine learning models for a lead time of 1 month in terms of different drought characteristics. The results from this work can be used for drought mitigation purposes and different models need to be tested to further enhance our capabilities.</p>





- Long Short Term Memory (LSTM) model was used to forecast short term drought.
- Drought index and predictor data used for the study were collected from CRU.
- Results were examined in terms of drought intensity and drought categories.

# 1 **An Improved SPEI Drought Forecasting Approach using the Long Short-** 2 **Term Memory Neural Network**

3 Abhirup Dikshit<sup>1</sup>, Biswajeet Pradhan <sup>1,2,3,4\*</sup>, Alfredo Huete<sup>1,5</sup>

4 <sup>1</sup>Centre for Advanced Modelling and Geospatial Information Systems (CAMGIS), University of  
5 Technology Sydney, NSW 2007, Australia; [abhirup.dikshit@student.uts.edu.au](mailto:abhirup.dikshit@student.uts.edu.au) (A.D.),  
6 [biswajeet.pradhan@uts.edu.au](mailto:biswajeet.pradhan@uts.edu.au) (B.P.)

7 <sup>2</sup>Department of Energy and Mineral Resources Engineering, Sejong University, Choongmu-gwan, 209  
8 Neungdong-ro, Gwangjin-gu, Seoul 05006, Korea

9 <sup>3</sup>Center of Excellence for Climate Change Research, King Abdulaziz University, P. O. Box 80234, Jeddah  
10 21589, Saudi Arabia

11 <sup>4</sup>Earth Observation Center, Institute of Climate Change, Universiti Kebangsaan Malaysia, 43600 UKM,  
12 Bangi, Selangor, Malaysia

13 <sup>5</sup>School of Life Sciences, Faculty of Science, University of Technology Sydney, Sydney, NSW 2007,  
14 Australia. [alfredo.huete@uts.edu.au](mailto:alfredo.huete@uts.edu.au) (A.H.)

15 Correspondence: Biswajeet Pradhan, [biswajeet.pradhan@uts.edu.au](mailto:biswajeet.pradhan@uts.edu.au)

## 16 **Abstract**

17 Droughts are slow-moving natural hazards that gradually spread over large areas and capable of  
18 extending to continental scales, leading to severe socio-economic damage. A key challenge is developing  
19 accurate drought forecast model and understanding a models' capability to examine different drought  
20 characteristics. Traditionally, forecasting techniques have used various time-series approaches and  
21 machine learning models. However, the use of deep learning methods have not been tested extensively  
22 despite its potential to improve our understanding of drought characteristics. The present study uses a  
23 deep learning approach, specifically the Long Short-Term Memory (LSTM) to predict a commonly used  
24 drought measure, the Standard Precipitation Evaporation Index (SPEI) at two different time scales  
25 (SPEI 1, SPEI 3). The model was compared with other common machine learning method, Random  
26 Forests, Artificial Neural Networks and applied over the New South Wales (NSW) region of Australia,  
27 using hydro-meteorological variables as predictors. The drought index and predictor data were  
28 collected from the Climatic Research Unit (CRU) dataset spanning from 1901-2018. We analysed the  
29 LSTM forecasted results in terms of several drought characteristics (drought intensity, drought  
30 category, or spatial variation) to better understand how drought forecasting was improved. Evaluation  
31 of the drought intensity forecasting capabilities of the model were based on three different statistical  
32 metrics, Coefficient of Determination ( $R^2$ ), Root Mean Square Error (RMSE), and Mean Absolute Error  
33 (MAE). The model achieved  $R^2$  value of more than 0.99 for both SPEI 1 and SPEI 3 cases. The variation  
34 in drought category forecasted results were studied using a multi-class Receiver Operating

35 Characteristic based Area under Curves (ROC-AUC) approach. The analysis revealed an AUC value of  
36 0.83 and 0.82 for SPEI 1 and SPEI 3 respectively. The spatial variation between observed and forecasted  
37 values were analysed for the summer months of 2016-2018. The findings from the study show an  
38 improvement relative to machine learning models for a lead time of 1 month in terms of different  
39 drought characteristics. The results from this work can be used for drought mitigation purposes and  
40 different models need to be tested to further enhance our capabilities.

41 **Keywords:** Standard Precipitation Evaporation Index; New South Wales; Drought Forecasting; Deep  
42 Learning

### 43 **1. Introduction**

44 Droughts are one of the most devastating natural hazards affecting various parts of the world. The  
45 phenomenon starts with the deficiency in rainfall, and it affects various aspects like stream-flow and  
46 soil moisture. The factors affecting or leading to droughts can be several ranging from meteorological  
47 parameters to climatic factors and even the effect of anthropogenic activities (Van Loon et al. 2016).  
48 Droughts can be broadly categorized as meteorological, which means the scarcity of rainfall beneath a  
49 certain truncation level; hydrological which refers to reduction in stream-flow; agricultural which leads  
50 to reduction in soil moisture content and ultimately crop yield; and socio-economic drought; which is  
51 the economic hardship faced by the people as a combination of all the above drought types. However,  
52 of late, several researchers have attempted to further categorize drought types, with Mishra and Singh,  
53 (2010) suggesting to add ground water drought; Vicente Serrano et al. (2019) suggesting environmental  
54 droughts as another category and a few suggesting to add ecological drought as a separate drought type  
55 (Slette et al. 2019). Among all these category types, one thing is for certain: that droughts are very  
56 complex and an international consensus on drought types is necessary.

57 Considering forecasting droughts, there are broadly three steps: i) defining a drought; ii) input data;  
58 and iii) models used. In terms of defining a drought, researchers have come up with several indices for  
59 different purposes which helps to understand various drought characteristics like onset, end, duration  
60 and intensity. These indices depend on the parameters being considered which could be a  
61 meteorological type, like Standard Precipitation Index (SPI) (McKee et al. 1993), derived from  
62 precipitation and typically used for meteorological droughts or Standard Precipitation Evaporation  
63 Index (SPEI) (Vicente Serrano et al. 2010; 2012), derived from precipitation and temperature and can  
64 be used for meteorological and/or hydrological droughts. Other drought indices type include derived  
65 from remote sensing products like Soil Adjusted Vegetation Index (SAVI) (Huete et al. 1988), which can  
66 be used to understand the vegetation aspects. Recently, Yihdego et al. (2019) presented a  
67 comprehensive list of the various drought indices used in the literature. As there have been over 150  
68 drought indices developed, validating everyone and developing a common consensus is not feasible.  
69 However, lately there seems to be a growing consensus about the use of SPEI, primarily because of its  
70 use of rainfall and temperature while determining index and not only rainfall as is the case in SPI.  
71 Therefore, SPEI was used in the present study due to its growing acceptability and its ability to use both  
72 rainfall and temperature parameters for calculation. The values are further categorized into different

73 levels of drought or non-drought conditions, which can be perceived as a reflection of the actual  
 74 conditions (Hao et al. 2016).

75 Several researchers have attempted to predict droughts at different lead times, with the aim of  
 76 increasing the forecasting capability at higher lead times. Another important aspect in drought studies  
 77 is the input data and the variables being considered for any analysis type. The input data can be  
 78 generally classified as ground-based or satellite based. The ground-based data could be further  
 79 categorised as station-based and interpolated grids (Sun et al. 2016). The interpolated gridded datasets  
 80 are based on gathering site-specific data from across the world and apply different interpolation grids  
 81 to produce a global/continental scale map of certain drought affecting variables (Sun et al. 2016). Such  
 82 datasets have the benefit of higher temporal resolution, which is crucial for drought studies. On the  
 83 other hand, remote sensing based datasets suffer from lower temporal resolution, which are not ideal  
 84 for forming a robust architecture for drought forecasting studies (Hao et al. 2018). Table 1 provides the  
 85 advantages and limitations of the data types, along with suggested review articles of the various  
 86 interpolated grids and remote sensing datasets.

87 Table 1. Advantages and limitations of the data types

<b>Data Type</b>	<b>Advantages</b>	<b>Limitations</b>	<b>Popular products</b>	<b>Review Article</b>
Ground based	<ul style="list-style-type: none"> <li>- Long time series data</li> <li>- Good for analysing drought sensitive regions</li> <li>- Can cover large areas (continental to global scale)</li> </ul>	<ul style="list-style-type: none"> <li>- Manual Errors</li> <li>- Need to check the homogeneity and fill the missing values in case of site-specific data</li> <li>- Depends on the interpolation techniques used</li> </ul>	<ul style="list-style-type: none"> <li>- Meteorological Stations</li> <li>- Interpolated Grids (CRU, Global Precipitation Climatology Centre (GPCC))</li> </ul>	Sun et al. (2018)
Remote Sensing	<ul style="list-style-type: none"> <li>- Information of vegetation data</li> <li>- Closely monitor the changes in agriculture</li> </ul>	<ul style="list-style-type: none"> <li>- Not available for enough duration</li> <li>- Low temporal resolution</li> </ul>	MODIS, Sentinel -1, 2, 3	West et al. (2020)

88

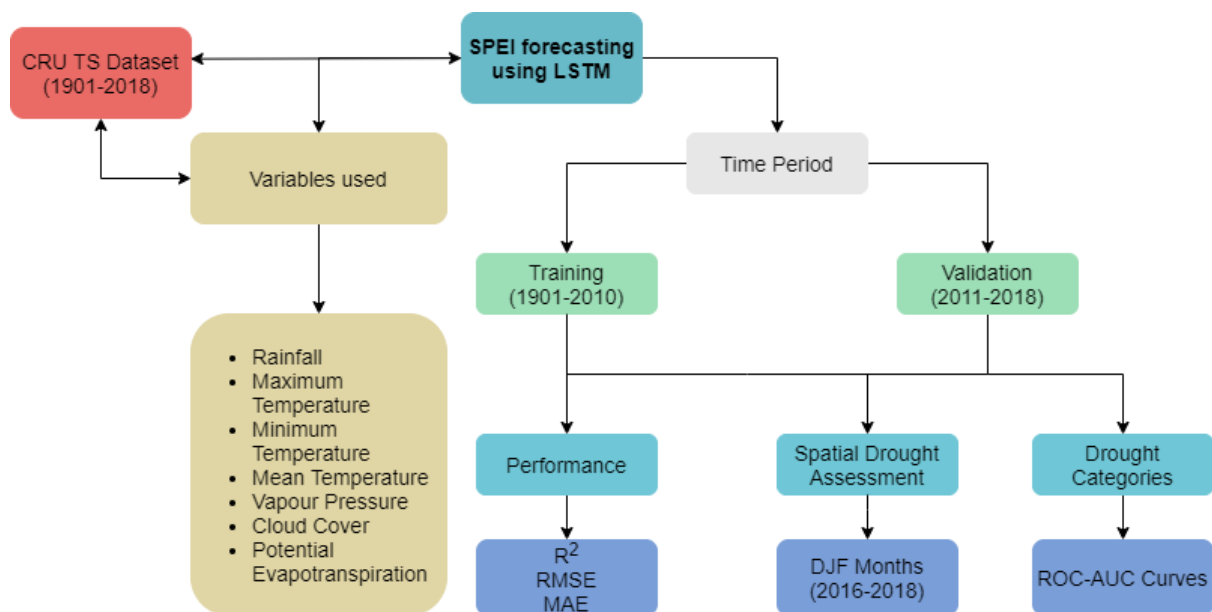
89 Using the climatological dataset for drought studies has seen a rise as more and more datasets are being  
 90 made available. Sun et al. (2018) reviewed 30 global precipitation datasets developed using various  
 91 approaches and found that the use of any dataset depends on the study area and the type of study being  
 92 performed. As precipitation is one of the key drought influencing factors and the present study is being

93 conducted on a considerably large area, we have used one of the most popular and well-accepted global  
94 climatological dataset, namely Climate Research Unit (CRU TS v 4.03) spanning from 1901-2018 at a  
95 spatial resolution of 0.5° (Harris et al. 2019; 2020). Further, the usability of CRU dataset for drought  
96 studies has been explored by several studies, like Vicente-Serrano et al. (2012) compared the  
97 performance of four different drought indices using CRU at a global scale; Spinoni et al. (2019) used  
98 CRU to prepare a global database of meteorological droughts. For NSW, the viability of the dataset for  
99 drought studies has been examined and verified by Dikshit et al. (2020a). The use of variables to  
100 accurately forecast meteorological drought has seen utilization of several factors like temperature,  
101 evapotranspiration and other factors like sea surface temperatures and climatic indices. The inclusion  
102 of climatic variables have shown to improve the forecasting results at higher lead times (6-12 months)  
103 (Özger et al. 2012), however, as the present work forecasts only at a lead time of 1 month, the use of  
104 local climate variables can be considered sufficient as highlighted in previous works (Mishra and Singh  
105 2011; Hao et al. 2018). The meteorological variables available from CRU dataset are precipitation,  
106 vapour pressure, cloud cover, potential evapotranspiration and temperature (mean, minimum and  
107 maximum).

108 And the final step depends on the forecasting model and the drought characteristics being analysed.  
109 The approaches used for drought forecasting can be classified into statistical (Deo and Sahin, 2015),  
110 physical (Hao et al. 2018) and hybrid (Wang et al. 2012) models. Statistical models analyses  
111 relationships among historical records, by considering various influencing factors as predictors.  
112 Physical based models involve the use of General Circulation Models (GCMs), which considers the  
113 physical processes between the atmosphere and land surface. Hybrid models involve the combination  
114 of both statistical and physical based models. In case of statistical models, various techniques like  
115 regression, time series analysis and machine learning approaches are used. The use of machine learning  
116 approaches, specifically, Artificial Neural Networks (ANN) have seen a rise, primarily due to the non-  
117 linear behaviour of droughts (Mishra and Singh, 2011). However, neural networks are incapable of  
118 dealing with non-stationarities in drought estimations and suffer from overfitting due to lag  
119 components involved in time series data (Alizadeh and Nikoo, 2018). Readers are referred to Mishra  
120 and Singh, (2011); Hao et al. (2018) and Fung et al. (2019) for a more detailed understanding of the  
121 various approaches used for forecasting purposes, along with their advantages and limitations.  
122 Therefore, there is a growing consensus to improve the forecasting abilities and one way to achieve it is  
123 by the use of deep neural networks which has shown tremendous capabilities to outperform the  
124 traditional approaches. Various fields like speech recognition (Hinton et al. 2012), self-driving vehicles  
125 (Farabet et al. 2012), computer vision (Krizhevsky et al. 2012) and natural language processing  
126 (Collobert et al. 2011) have immensely benefitted. In the case of droughts, deep learning has been used  
127 to forecast sea surface temperatures using hybrid Long Short-Term Memory (LSTM) technique (Xiao  
128 et al. 2019); developing drought monitoring tool using deep feed forward neural network (Shen et al.  
129 2019); drought index forecasting (SPEI, SPI) using LSTM (Poornima and Pushpalata, 2019). The study  
130 by Poornima and Pushplata, (2019) used a variety of local climatic variables to forecast SPEI and SPI  
131 for a temporal range of 1980 to 2013 for a single site in Hyderabad, India. The model was able to achieve  
132 accuracy of 97% and 99% for monthly SPEI and SPI, respectively. Their study used ground-based data



133 and the temporal range used was 1980 to 2013. The use of relatively shorter time scale may hinder to  
 134 adequately capture patterns and depict more reliable results. Therefore, the present study aims to use  
 135 LSTM technique using global climatological dataset to understand the forecasting capabilities in terms  
 136 of SPEI values and analysing the variation in terms of drought categories and spatial variation. The  
 137 model was trained from 1901-2010 providing it with sufficient data to learn the relationship between  
 138 drought index and the causative factors. Next, the model was validated from 2011-2018 and the results  
 139 were analysed at 1 month lead time. In summary, the present work aims to achieve three main  
 140 objectives: i) How well can deep learning models forecast meteorological drought?; ii) Understanding  
 141 the spatial variation between observed and predicted values; and iii) Examining the variation in terms  
 142 of drought categories as defined by index values. The flowchart of the study is illustrated in Figure 1.



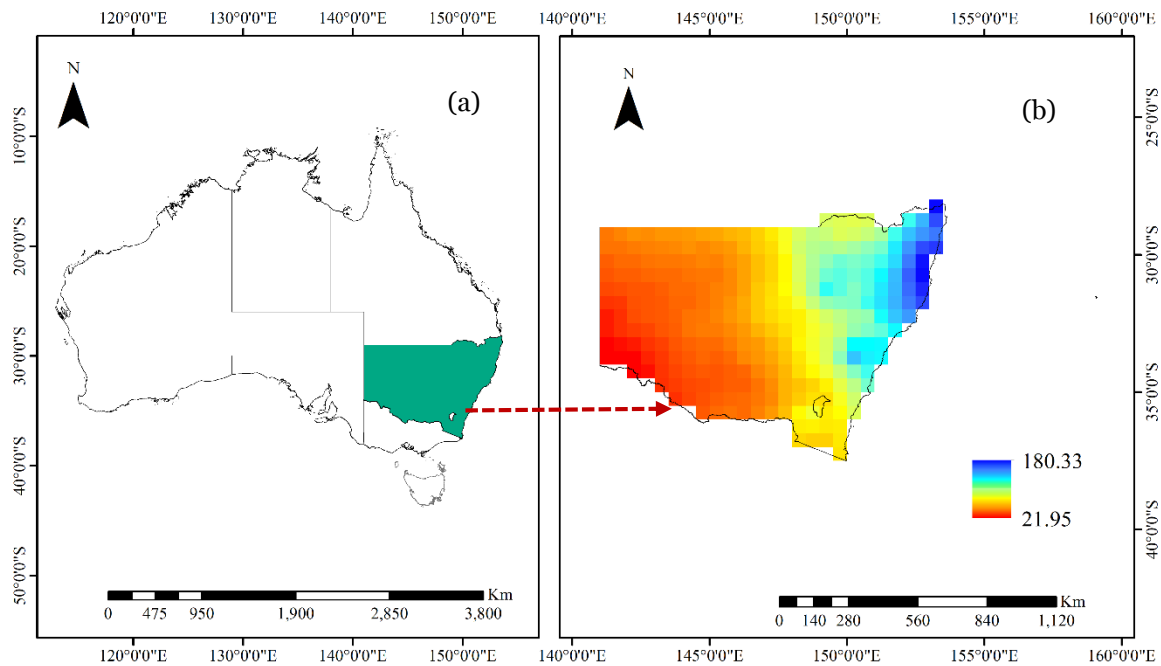
143

144 **Figure 1.** Flowchart of the study conducted in this research.

145 **2. Study Area**

146 The area of interest for the present work is New South Wales (NSW) which is in the south-western part  
 147 of Australia (Figure 2). The region has a history of droughts that have led to huge economic loss in terms  
 148 of agricultural production, water availability, and social distress (Pittock et al. 2015). The Bureau of  
 149 Meteorology (BoM), Australia has classified the region into four different climatic zones, wherein most  
 150 of the region suffers from hot dry summer and cold winters. The three hottest months or the summers  
 151 typically start in December and ends in February. The region encompasses an area of around 800,400  
 152 km<sup>2</sup> with a population of 7,861,700 (ABS, 2018). Around 81% of the region falls under agricultural land,  
 153 and 14% of the region is classified as protected areas. The most common land use by area is grazing  
 154 native vegetation, which is roughly 44% of the state (ABARES, 2016). From 1900, the region has  
 155 suffered from three major droughts [(Federation Drought (1895-1902), World War II (1937-1945) and  
 156 Millennium (2001-2010)] and several minor droughts (Dikshit et al. 2020b). Wittwer, (2020) estimated  
 157 the economic impact due to droughts from 2017-2019, and found that a total of 8.1 Billion\$ was lost

158 during this period. The Millennium Drought which is considered being the worst drought in history,  
159 had led to several social issues like enforcing water restrictions in major cities, an increase in electricity  
160 prices, and also a major contributor to bushfire events in 2003 and 2009 (Van Dijk et al. 2013). Further,  
161 the drought was considered as the leading factor for a clear reversal in water cycle intensification  
162 observed in previous years (Huntington, 2006). Also, the recent bushfires in 2019 have been found to  
163 be further aggravated due to the combination of drought conditions, dry vegetation and rise in  
164 temperature (Steffen et al. 2019; Nolan et al. 2020).



165

166 **Figure 2.** Location of the study area and the long-term mean rainfall map based on the base period of  
167 1961-1990 calculated from CRU-TS dataset.

168 As explained in the introduction section, the understanding of the drought is quite varied and its  
169 definition for characteristics like onset and end is also different. As an example, BoM defines drought  
170 onset, when precipitation is below 10<sup>th</sup> percentile and as serious when precipitation is below 5% of  
171 observations, however a clear definition marking the cease of drought has not been defined (Heberger,  
172 2012). However, the Department of Primary Industries, NSW uses Combined Drought Index (CDI) as  
173 a drought indicator, which combines meteorological, hydrological and agronomic definitions of drought  
174 using indexes for rainfall, soil water and plant growth and drought direction. Therefore, to avoid such  
175 confusion, we used the globally accepted SPEI drought index as an indicator to forecast drought index.  
176 In terms of climatic variation, the region has seen an increase in the intensity and frequency of hot days  
177 and heat waves in Australia, exacerbating drought conditions (Cai et al. 2012), with a decrease in rainfall  
178 since 1950 (Dey et al. 2019).

### 179 **3. Drought Index and Data Used**

180 The data used for the present study is Climatic Research Unit (CRU TS v 4.03) dataset developed by the  
 181 University of East Anglia at 0.5° x 0.5° spatial resolution from 1901-2018 (Harris et al. 2019; 2020).  
 182 The dataset has been used for various purposes like climate variability, paleo-climatic (Nagavciuc et al.  
 183 2019) and agronomic studies (Renard et al. 2019). In total, the dataset provides ten different variables  
 184 which can be either primary, secondary or derived. The variables used in the present study are primary  
 185 variables that include precipitation and mean temperature; secondary variables are vapour pressure  
 186 and cloud cover; and derived variables are potential evapotranspiration, minimum and maximum  
 187 temperature.

### 188 3.1 Standard Precipitation Evaporation Index

189 The Standard Precipitation Evaporation Index (SPEI) is one of the most commonly used drought index  
 190 for forecasting purposes after its introduction by Vicente Serrano et al. (2010). This is primarily due  
 191 to its dependency on both rainfall and temperature data, unless like SPI, which only uses rainfall data.  
 192 The calculation of SPEI includes determining “climatic water balance” which involves the use of rainfall  
 193 and potential evapotranspiration. The calculation of SPEI can be conducted at various time scales,  
 194 ranging from 1 month to 24 months, which depicts different drought type (Vicente Serrano et al. 2010).  
 195 To calculate SPEI index at different time scales ( $n = 1, 3$ ), the monthly climatic water balance series is  
 196 aggregated with an  $n$ -month moving sum, i.e. the current monthly value and the previous  $n - 1$  monthly  
 197 values. Like, a 3-month accumulation data for January–February–March determines the index for the  
 198 month of March (Vicente Serrano et al. 2010). The climatic water balance is computed at different time  
 199 scales, and the resulting values are fitted to a log- logistic probability distribution to transform the  
 200 original values to standardized units (Beguería et al. 2014). Generally, the shorter time scales (1-3  
 201 months) represent the meteorological drought, whereas 3-6 month time scale describes agricultural  
 202 drought, while a larger time scale, 12-24 months is suitable to describe hydrological drought (Mishra  
 203 and Singh, 2010). As meteorological droughts can be considered as the first step in drought evolution,  
 204 the present study, forecasts SPEI at 2 different time scales (SPEI 1 and SPEI 3). Interested readers are  
 205 referred to Vicente Serrano et al. (2010; 2012) for a detailed study about the calculation of SPEI drought  
 206 index. The global SPEI database at different monthly scales using the CRU dataset can be accessed from  
 207 <https://spei.csic.es/database.html>. Table 2 represents the various drought categories as per SPEI index  
 208 values.

209 **Table 2:** Drought categories as per SPEI values (Rhee and Im, 2017)

SPEI Classifications	Categories
$\leq -2.0$	Extremely Dry
-1.99~-1.5	Severely Dry
-1.49~-1.0	Moderately Dry
-0.99~0.99	Near Normal
1.0~1.49	Moderately Wet
1.5~1.99	Severely Wet
$\geq 2.0$	Extremely Wet

210

#### 211 **4. Recurrent Neural Networks and LSTM Model**

212 Deep learning as a distinct field has emerged to reduce human effort in traditional machine learning  
213 (ML) approaches for various tasks like feature extraction and regression purposes (LeCun et al. 2015).  
214 Typically, ML models have some level of human input which makes it difficult to understand complex  
215 situations and therefore, deep learning which does not involve human input became more prominent.  
216 Although, the concept of deep learning can be tracked back to 1950, it resurrected itself after defeating  
217 humans in the game of Go, which was one of the biggest achievement in the recent time (Silver et al.  
218 2016). Further, the detailed review of deep learning, LeCun et al. (2015) gave new directions to various  
219 research fields and has been adopted in respective domains. There have been several milestones  
220 achieved in deep learning in the past decade, each achieving new feats in their respective fields  
221 (Schmidhuber, 2015). However, the traditional computer vision field is slightly different from  
222 geohazards or geosciences applications as the latter involves a dynamic component which is not the case  
223 in the former (Reichstein et al. 2019). Also, the availability of various types of data include remote  
224 sensing, atmospheric or climatic data has led researchers to use different approaches with a definite  
225 aim like forecasting or monitoring.

226 Of the various deep learning based approaches, Recurrent Neural Networks (RNN) is a neural network  
227 type which is used to understand non-stationary data like time series data. It can be considered as a  
228 series of interconnected networks for time series analysis and can be trained using back propagation  
229 based gradient descent algorithms (Williams and Zipser, 1989). The ability to consider both the current  
230 and preceding input data for mapping target vectors in RNN makes it useful compared to neural  
231 networks, which map target vectors by multiplying weights. Also, RNN has the ability to store an  
232 internal memory of previous inputs in the network, which allows it to recall key events that occurred  
233 several times in the past, which is key in studies like drought forecasting. The scenario where RNN fails  
234 is when stacking occurs leading to vanishing and exploding gradient problems (Bengio et al. 1994). This  
235 led to the introduction of long short-term memory (LSTM) (Hochreiter and Schmidhuber, 1997), which  
236 comprised of a cell capable of storing the values to be used at random intervals and three gates, viz.,  
237 input, output and forget gate, to control and adjust the cell state.

238 The structure of LSTM is like a chain as shown in Figure 3, wherein the basic building block is a cell and  
239 its state is the key to the mode. There are three types of gate which determines the cell state, which  
240 includes an input, forget gate and an output gate. The gates analyse and control the amount of  
241 information it can pass through and are comprised of a sigmoid neural layer and point-wise  
242 multiplication operation (Olah, 2015). The working mechanism of the gates and information flow can  
243 be expressed using the following equations:

$$244 \quad f_t = \sigma(W_f \cdot [h_{t-1}, x_t] + b_f) \quad (1)$$

$$245 \quad i_t = \sigma(W_i \cdot [h_{t-1}, x_t] + b_i) \quad (2)$$

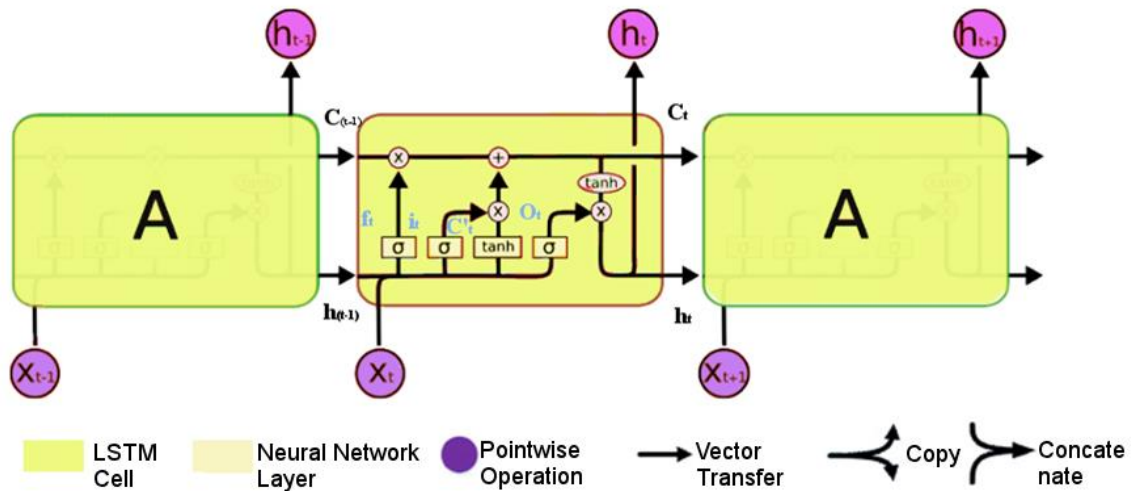
246 
$$C'_t = \tanh(W_c \cdot [h_{t-1}, x_t] + b_c) \quad (3)$$

247 
$$C_t = f_t * C_{t-1} + i_t * C'_t \quad (4)$$

248 
$$o_t = \sigma(W_o \cdot [h_{t-1}, x_t] + b_o) \quad (5)$$

249 
$$h_t = \sigma_t * \tanh(C_t) \quad (6)$$

250 Where  $x_t$  is the input vector at time  $t$  with  $\sigma$  being the activation function like *Sigmoid* or *ReLU*.  $W_f$ ,  $W_i$ ,  
 251  $W_c$  and  $W_o$  are the applied weights to concatenation of the new input  $x_t$  and output  $h_{t-1}$  from the  
 252 previous cell, with  $b_f$ ,  $b_i$ ,  $b_c$ , and  $b_o$  being the corresponding bias (Xiao et al. 2019).  $f_t$ ,  $i_t$ , and  $o_t$  are the  
 253 outputs of three sigmoid functions  $\sigma$ , and the values range from 0 to 1. These control the information  
 254 which are forgotten in the old cell state  $C_{t-1}$  and passed to the new cell  $C_t$  with the new information  
 255 being  $C'_t$ , with  $h_t$  being the output information from the cell. There are several variants of LSTM and  
 256 interested readers can refer to Goodfellow et al. (2016).



257

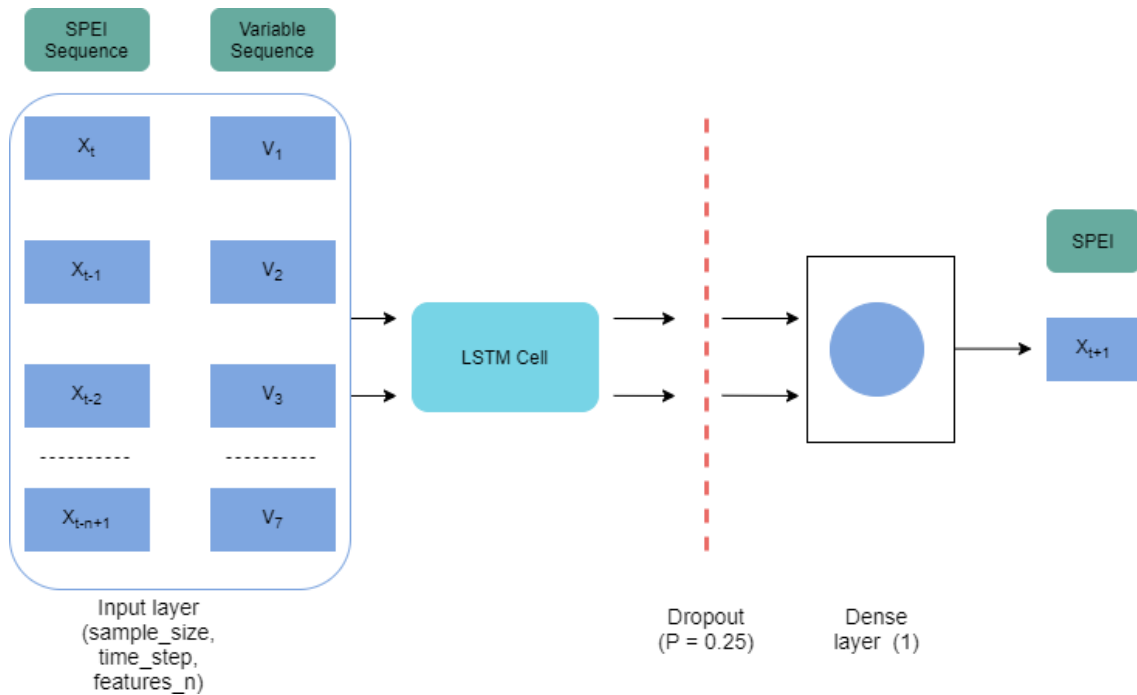
258 **Figure 3.** Structure of LSTM network (Olah, 2015).

259 The LSTM model used for SPEI forecasting, is depicted in Fig. 4. It consists of an input layer, one LSTM  
 260 layers and one Dense layer (also known as fully connected layers). We have conducted several  
 261 experiments and found that this architectural design achieves the best prediction performance. The  
 262 input of the whole network is in 3D tensor form and expressed as [sample\_size (1901-2010),  
 263 time\_steps, features\_n (7)]. Sample\_size is the training data, and is set to 2010. time\_steps is the size  
 264 of the time window (previous months) used to predict the SPEI. As there is no fixed rule for portioning  
 265 the data, the most commonly used approach is to split the data into two sets (Mokhtarzad et al. 2017).  
 266 Further, the amount of data in the training set has also no set rule, therefore, the present work uses 90%  
 267 of the dataset as training (Deo et al. 2017b; Dikshit et al. 2020b). Therefore, training data is set to 2010  
 268 and the remaining as validation. The choice of the time steps was set to 20, based on a trial-and-error  
 269 approach and running several experiments (time\_step = 5, 10, 15,...50). This means that the  
 270 parameters from the past 19 months also including the 20<sup>th</sup> month parameters was used to predict the

271 21<sup>st</sup> month's SPEI. As we use SPEI values as predictors, based on multiple involved factors, we set the  
 272 feature\_n to the number of involved factors, i.e., 7. A dropout mechanism is applied to the inputs to  
 273 help prevent over-fitting during training, which is empirically set to 0.25 (Xiao et al. 2019). For  
 274 regression task, the input data is normalized to the range of [0 1] using the following algorithm:

$$275 \quad X_{nor} = \frac{(Y_{max} - Y_{min}) * (X - X_{min})}{(X_{max} - X_{min})} + Y_{min} \quad (7)$$

276 Where  $X$  is the value to be normalized;  $X_{nor}$  is the normalized  $X$  value;  $Y_{max} = 1$ ;  $Y_{min} = 0$ ;  $X_{max}$  and  $X_{min}$   
 277 are the maximum and minimum value of each time series respectively. The LSTM deep neural network  
 278 is implemented with Keras (Francois, 2015) utilizing TensorFlow 2.0 (GPU version) as the backend.



280 **Figure 4.** Architecture of the LSTM network for SPEI forecasting.

281 The design of the architecture was initially conducted for SPEI 1 case. Later, similar approach was used  
 282 for SPEI 3 case, however, the change in metrics was minimal, and therefore, both SPEI 1 and SPEI 3  
 283 have the same architecture. After training the data, the predicted images for SPEI 1 SPEI 3 at one month  
 284 lead time are generated to analyse the spatial variation. The analysis was conducted at different seasonal  
 285 level to examine how the model performs, which would give more clarity about the model's capability.  
 286 The performance of the model was examined using various approaches and the details are presented  
 287 below.

#### 288 4.2. Performance metrics

289 The performance metrics was based on three different statistical metrics for analysing the forecasted  
 290 results at different lead times. The metrics used were Coefficient of Determination ( $R^2$ ) and Root Mean  
 291 Square Error Method (RMSE). The mathematical formulae to the metrics are:

292 
$$R^2 = \frac{\sum_{i=1}^N (\hat{y}_i - \bar{y}_i)}{\sum_{i=1}^N (y_i - \bar{y}_i)^2}, \quad (8)$$

293 
$$\bar{y}_i = \frac{1}{N} \sum_{i=1}^N y_i, \quad (9)$$

294 where,  $\bar{y}_i$  is the mean value,  $y_i$  and  $\hat{y}_i$  are observed and forecasted values, N being the number of data  
 295 points.

296 
$$RMSE = \sqrt{\frac{SSE}{N}}, \quad (10)$$

297 
$$SSE = \sum_{i=1}^N (\hat{y}_i - y_i)^2, \quad (11)$$

298 where, SSE refers to sum of squared errors.

299 RMSE is frequently used as an evaluation metric as it penalises large errors and is suitable for time  
 300 series forecasting purposes.  $R^2$  represents the extent of association between the observed and forecasted  
 301 values. The value ranges from 0 to 1, where 1 indicates an exact match and 0 denotes no association. By  
 302 contrast, a lower RMSE value depicts better performance. Mean Absolute Error (MAE) determines the  
 303 average of absolute errors, analysing the degree of proximity of forecasted values with the observed  
 304 values.

305 As the study also aimed to analyse the drought class (Table 2) of the forecasted results, a multi class  
 306 Receiver Operating Characteristic based Area under Curve (ROC-AUC) approach was used. This  
 307 approach determines the sensitivities and specificities at all the thresholds which are defined as per the  
 308 response of the classifier for a test set which is followed by AUC computation using the trapezoid rule  
 309 (Buda et al. 2018). The traditional use of these curves revolves around binary classification works,  
 310 therefore, we implemented a multi-class ROC (Provost and Domingos, 2003) to address the various  
 311 drought classes and the imbalances associated with it. We used the scikit-learn python package to  
 312 implement the technique (Pedregosa et al. 2011). The methodology included the determination of  
 313 statistical metrics for every class and thereby averaging the results. The average of the results can be  
 314 done either using micro or macro averages. Generally, for a multi class classification problem with class  
 315 imbalance case, as is the present study, micro-average is to be preferred (Van Ash, 2013). This is due to  
 316 the principle behind computation of these averages. A micro average aggregates the contributions of all  
 317 classes to compute the average metric, whereas a macro average would calculate the metric  
 318 independently for each class and then compute the average. So, the methodology involves the use of a  
 319 performance table as shown in Table 3.

320 **Table 3.** Performance table for occurrences labelled with class label X (Van Ash, 2013).

	<b>True label (X)</b>	<b>True not (X)</b>
<b>Predicted label (X)</b>	True Positive (TP)	False Positive (FP)
<b>Predicted not (X)</b>	False Negative (FN)	True Negative (TN)

321 The calculation of AUC for any class involves determining the Sensitivity and 1- Specificity. Sensitivity  
 322 is defined as:  $TP/TP + FN$ ; whereas Specificity is defined as:  $TN/TN + FP$ . The mathematical formulae  
 323 for determining the micro-average AUC is (Pedregosa et al. 2011):

$$324 \quad \text{Micro average} = \frac{2}{a(a-1)} \sum_{j=1}^a \sum_{y>x}^a (AUC(x|y) + AUC(y|x)) \quad - (12)$$

325 where  $a$  is the number of classes and  $AUC(x|y)$  is the AUC with class  $x$  as the positive class and class  $y$   
 326 as the negative class.

## 327 5. Results and Discussion

328 At first, the statistical metrics of the regression aspect was computed as shown in Table 3. The results  
 329 reveal excellent results during both the periods, thus affirming its superiority over traditional machine  
 330 learning models based on previous works conducted in NSW. Deo and Şahin, (2015) used Artificial  
 331 Neural Networks (ANN) and climatic indices to forecast monthly SPEI at five NSW locations and  
 332 achieved  $R^2$  values of  $\sim 0.99$ . However, the present study did not use climatic indices as predictors and  
 333 achieved similar results, thereby showing the benefits of using deep learning model over traditional  
 334 machine learning models. Dikshit et al. (2020b) used Random Forests model to predict SPEI 1 and SPEI  
 335 3 for NSW region, and the  $R^2$  value achieved was 0.73 and 0.76 respectively. Also, Deo et al. (2017a)  
 336 used a multivariate adaptive regression splines (MARS) model to forecast SPI for five different regions  
 337 of NSW, and the  $R^2$  value achieved ranged from 0.971-0.987. The forecasted results are examined in  
 338 two different ways: a) Spatio-temporal variation b) Variation in terms of drought categories. As it is not  
 339 feasible to depict the variation for every month, we highlight the spatio-temporal variation for the  
 340 summer months (December – January – February) from 2016-2018. As summer months are a period  
 341 of high temperature and low rainfall, and an analysis for this period can be considered as a good  
 342 estimate of the forecasting abilities for other time periods, either based seasonally or on months. The  
 343 variation at 1 month lead time between original and predicted SPEI 1 (Figure 5) and SPEI 3 values for  
 344 NSW region are illustrated in Figure 6.

345 **Table 4.** Statistical metrics of LSTM model under training and validation period.

Predicting	Training			Validation		
	$R^2$	RMSE	MAE	$R^2$	RMSE	MAE
SPEI 1	0.998	0.013	0.012	0.996	0.018	0.01
SPEI 3	0.997	0.016	0.014	0.992	0.027	0.024

346

### 347 5.1 Spatio-temporal variation

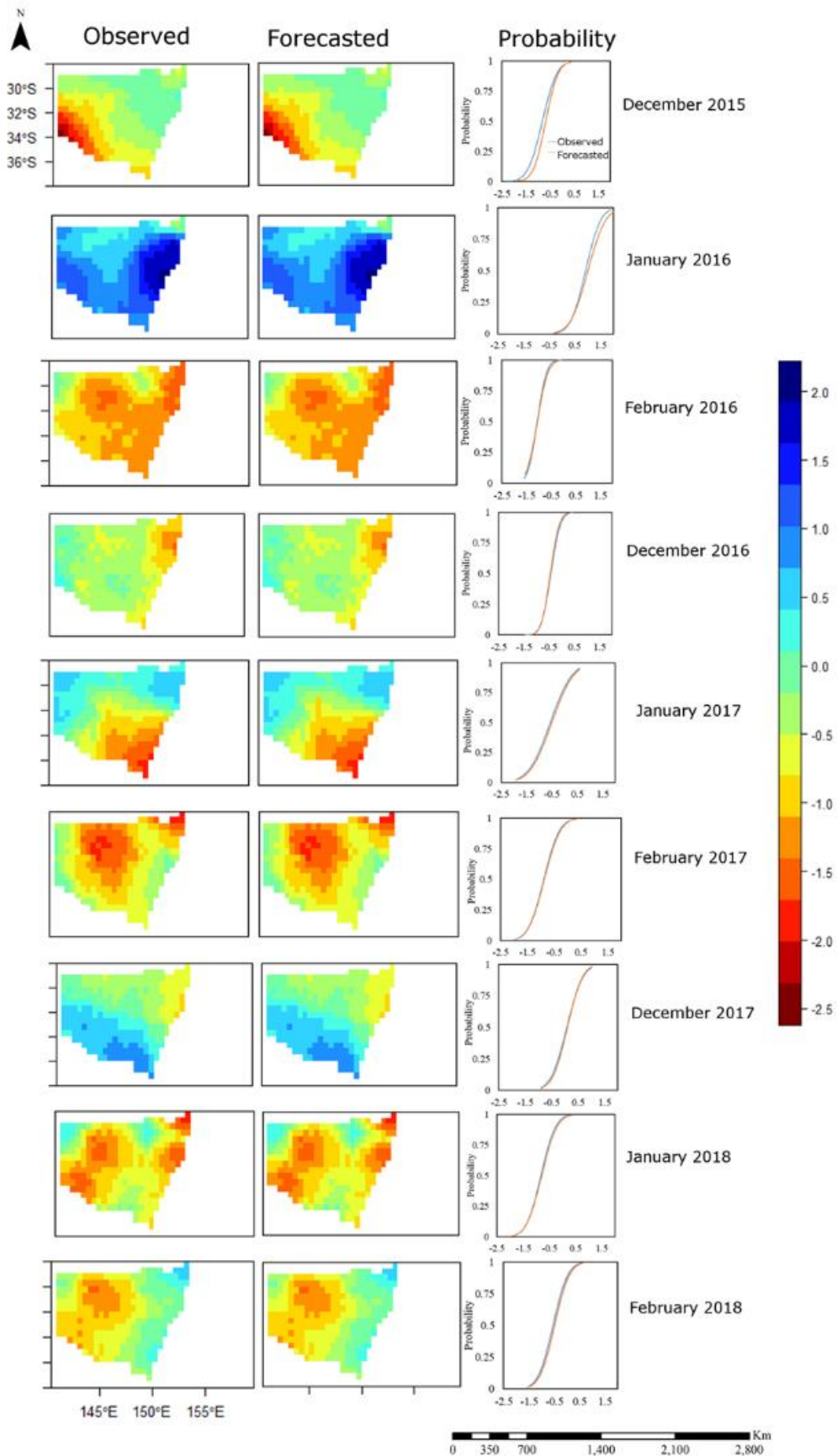
#### 348 5.1.1 SPEI 1 values

349

350 The observed SPEI 1 values during December 2015 depict very few regions with extremely dry  
 351 conditions towards the south-west part, and the following month shows no drought conditions with the  
 352 majority of the region depicting moderately to severely wet conditions. However, situations change in



353 February 2016, wherein the spatial extent of drought increases and 37.7% of the area comes under  
354 drought. Now, when analysing the summer of 2017, the month of December depicts few regions (5.8%),  
355 particularly, the northern-part under drought, but the drought increases towards severely dry  
356 conditions in January engulfing the south-eastern region and then further intensifying in February with  
357 the drought regions more towards the central and northern part of NSW. Similarly, in the summer of  
358 2018, the month of December showed no drought conditions, whereas January depicted areas with  
359 severe drought conditions, and the effect decreased in February. This would help to understand how  
360 the drought propagates within a region on a monthly scale. Now, on comparing with the predicted SPEI  
361 1 maps, the spatial variation in terms of values and categories is similar to observed maps. Also, the  
362 number of pixels under drought conditions ( $SPEI < -1$ ) is nearly 3%-5% more across the same months  
363 and under non drought conditions ( $SPEI > 1$ ) are less than the observed. This can be considered as a  
364 good step, as over prediction to a certain extent is good and could be helpful for policy makers. Similarly,  
365 for December 2017, the SPEI 1 values indicated no indication of drought and can be considered as near  
366 normal condition. However, in January 2018, the reduction in rainfall lead the western part of the area  
367 to come under severe drought. Also, almost 80% of the region was under some sort of drought category.  
368 The situation eases a little in February 2018, with the north and north-western part of the region under  
369 moderately dry condition. When comparing with the predicted images for the summer of 2018, the  
370 month of December leads to consistent results with the observed, and so is the case with the month of  
371 January. However, for February 2018, the area under drought is over predicted by 8% with some pixels  
372 depicting severely dry conditions.



373

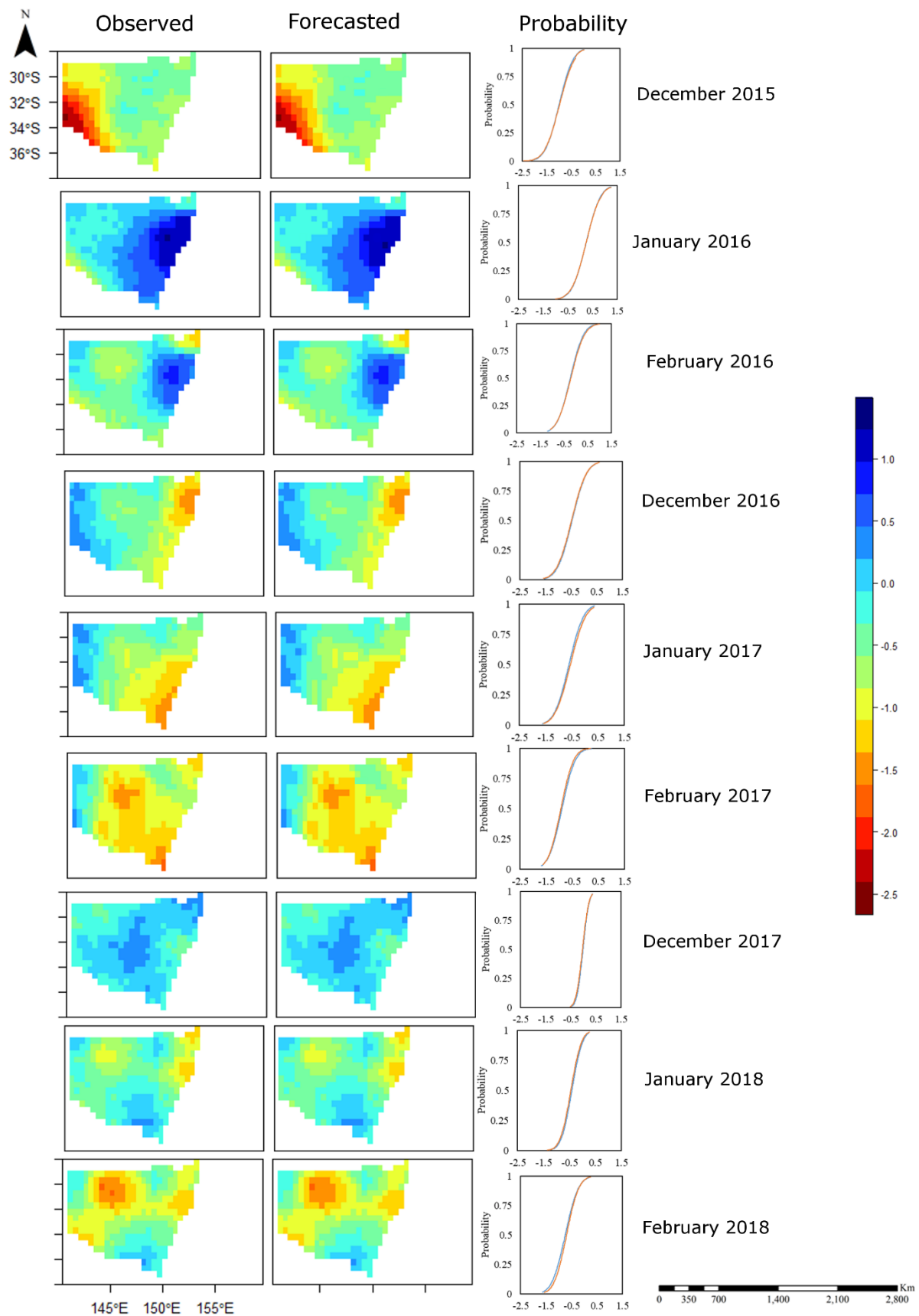
374 **Figure 5.** Spatial variation of SPEI 1 among the DJF (December – January – February) months of  
 375 2016-2018. The first column depicts the observed SPEI 1 values, second column depicts the predicted

376 index values. In the third column depict the probability (cumulative distribution function) plots of  
377 observed and forecasted values – of SPEI 1.

### 378 *5.1.2 SPEI 3 values*

379 For SPEI 3 case, the index value for December 2015 depicted the western part to be under severe  
380 drought (5.4%), with the conditions easing in the following month, with no region under drought.  
381 However, the month of February depicted very few pixels under drought (1.9%) in the northern part.  
382 The month of December in 2016 depicts most of the region as under near-normal conditions, whereas  
383 certain regions exhibited moderately dry conditions in the northern part, with few pixels highlighting  
384 severely dry conditions. The drought intensity for severely dry condition was less, and generally, the  
385 area was not under drought influence. Thereafter, January 2017 highlighted more drought areas with  
386 more regions exhibiting moderately-dry and severely-dry conditions, especially towards the south-  
387 eastern part. Further, in February 2017 the drought conditions expand to more areas, with more regions  
388 depicting moderately and severely dry conditions. Now, when we compare this with the predicted  
389 images, the range of index values as per drought class is generally same across summer of 2017, however  
390 the number of pixels under drought were over estimated by 4.5% in December 2016, under predicted in  
391 January and February 2017 by 3.7% and 5.6% respectively. Also, when analysing in terms of clusters for  
392 drought pixels, the variation is not significant enough and follows same trend.

393 The index values during December 2017 depict near normal conditions across the state, which leads to  
394 moderately dry conditions for January 2018, especially in the northern part of NSW and the drought  
395 intensifies to severe category and moves to further west in February 2018. On comparing it with the  
396 predicted images, the month of December 2017 shows similar conditions, and as the area was in near  
397 normal conditions, the variation in index value per pixel is not important. Further, for January 2018  
398 the number of pixels under drought is more than observed, but the values have been over predicted by  
399 6.4%, with a few of the pixels (2.4%) depicting moderately dry conditions, when the observed did not  
400 depict any drought. Similar is the condition for February 2018, which was under predicted by 3.6%.

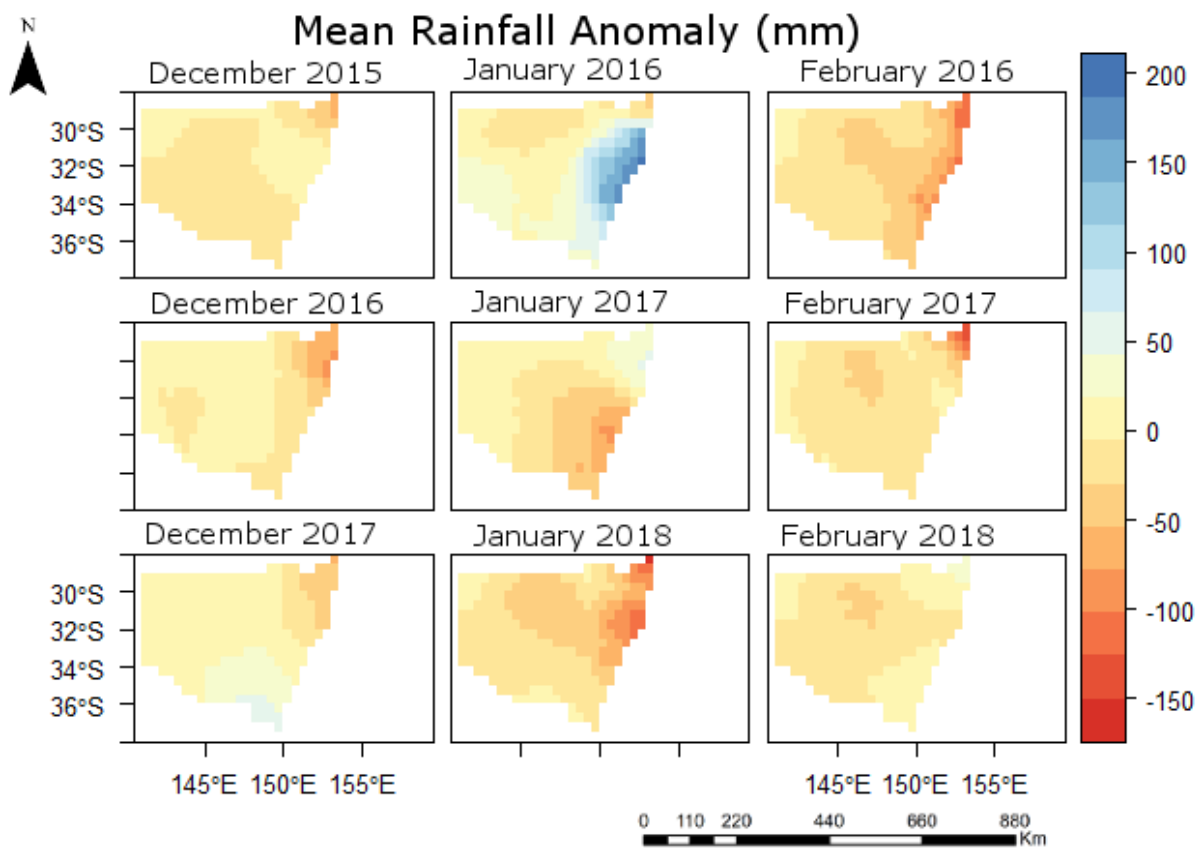


401

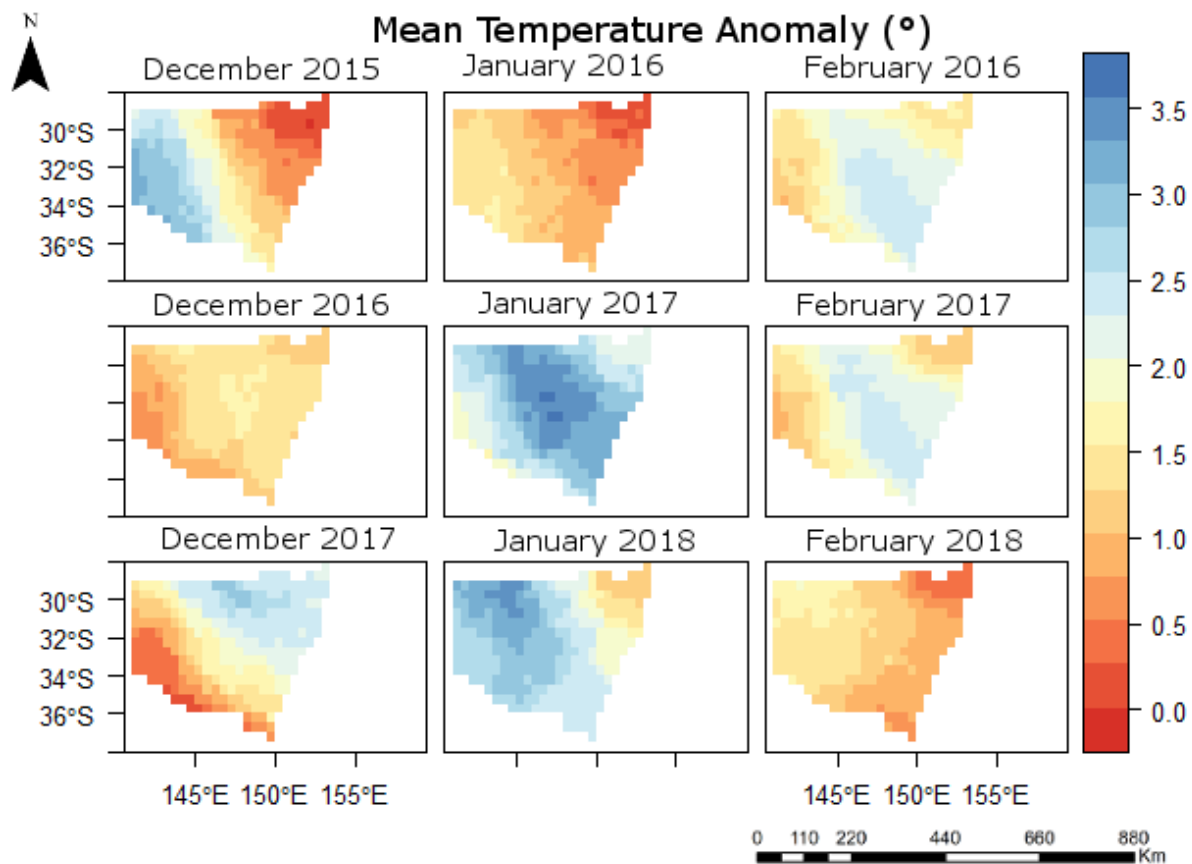
402 **Figure 6.** Spatial variation of SPEI 3 among the DJF (December – January – February) months of  
 403 2016-2018. The first column depicts the observed SPEI 3 values, second column depicts the predicted

404 SPEI 3 values. Legends represent drought index values. The third column depicts the probability  
405 (cumulative distribution function) plots of observed and forecasted SPEI 3 values.

406 To examine the importance of the LSTM architecture, annual rainfall and annual mean temperature  
407 anomaly maps are shown in Figures 7(a) and 7(b), with the baseline period as 1961-1990. For forecasting  
408 purposes, ML models learn uniform weights, whereas LSTM models learn variable weights across time  
409 steps. As the figure suggests, a significant variation in rainfall and temperature anomalies is observed  
410 during the summer periods of 2016-2018. This phenomenon necessitates the use of decay over weights  
411 across periods. Hence, the use of LSTM is encouraged to learn decayed weights. The forget gate in LSTM  
412 ensures that the model can effectively capture the decay weighted lag-lead sequence relationship  
413 without the vanishing gradient problem.



414



415

416 Figure 7. Spatial anomaly maps of (a) rainfall; and (b) mean temperature during the summer months  
 417 of 2016-2018

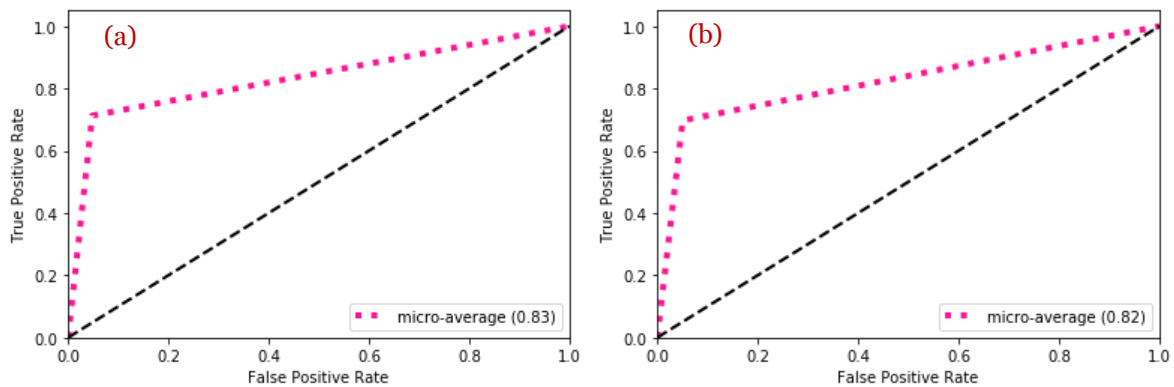
418 Further, on examining the variation between SPEI 1 and SPEI 3, an interpretation study was conducted  
 419 to understand the difference among the weights learned by variables. The results indicate that in case  
 420 of SPEI 1, the most dominant factor was rainfall, however, temperature was most dominant for SPEI 3.  
 421 The influence of vapour pressure and cloud cover were relatively similar for both the scenarios, but were  
 422 more influential than PET. This suggests that cloud cover and vapour pressure also play a key role, and  
 423 their inclusion can improve forecasting results. Further, in order to examine the spatial variation  
 424 between variables and drought index, a Convolutional Neural Network based LSTM (CNN-LSTM)  
 425 architecture, would be well suited. The recent study by Ham et al. (2019) to forecast El Niño/Southern  
 426 Oscillation (ENSO) index used such architecture to identify the hotspots of the variables, along with  
 427 forecasting at multi-year lead times.

## 428 5.2 Drought Classification

429 The above discussion reflects how the drought movement occurs at monthly scales and also during  
 430 different summer seasons. The key to understand the difference is the spatial variability depicting the  
 431 index values and also the drought category it represents. When we analysed the observed and predicted  
 432 images, there was minor variation in the index values, but represented different drought classes. For  
 433 SPEI 1 case, the observed value of February 2017 showed a maximum index value of -1.99 which is the  
 434 borderline for severely dry condition, however, for the same period, the predicted value depicted

435 maximum value of -2.08, which comes under severely dry condition. Similar was the case for February  
436 2018, wherein the predicted value depicted a higher drought class as compared to the observed value.  
437 This was also the case for SPEI 3 condition, December 2016, observed as severely dry condition whereas  
438 predicted fell under moderately dry condition. Therefore, there can be few scenarios where statistics  
439 may not be able to reveal drought class, due to the proximity between them.

440 The variation was analysed by computing the micro average of ROC based AUC curves. The results  
441 reveal that under both SPEI 1 and SPEI 3; the model achieved a value of 0.83 and 0.82, respectively  
442 (Figure 8). This proximity along the borderline of drought category has led to slightly lower values of  
443 AUC curves. However, when considering all the classes, the micro average from the present study  
444 outperforms the previous studies. This suggests that even though the statistical metrics provide  
445 excellent results, the understanding of droughts cannot be based only on such metrics, instead it should  
446 be based on the objective of the study. Moreover, the results achieved in the present work can be  
447 considered quite acceptable given that a formidable mitigation strategy for 1 month lead time can be  
448 developed.



449

450 **Figure 8:** ROC-AUC curves of different drought categorization classes (a) SPEI 1, and (b) SPEI 3.6.

## 451 **Conclusion**

452 Droughts are one of the most destructive hazards causing severe economic and social distributions. One  
453 of the most effective ways to understand droughts is to improve the existing forecasting ability. As the  
454 onset of drought is not clearly defined, forecasting of droughts make a compelling argument to improve  
455 the models providing better mitigation strategies. The present work uses a deep learning approach,  
456 namely LSTM, which has proven to be more effective for forecasting purposes compared to traditional  
457 machine learning approaches. The study forecasts SPEI drought index for New South Wales region  
458 determined using the global climatological dataset (CRU TS v 4.03) using seven different meteorological  
459 variables also collected from CRU dataset. The predictor and variables were collected from 1901-2018  
460 of which 1901-2010 were used as training data and then validated from 2011-2018. Apart from  
461 understanding the variation in pixel values, it is equally important to analyse under different drought  
462 characteristics, therefore a multi class ROC-AUC curves was prepared to understand the changes in  
463 terms of drought classes. In the present work, we focussed towards examining the model in terms of  
464 drought categories, which could be essential for mitigation purposes, especially when studying for a

465 large area. This is the first study in the use of a deep learning approach utilizing a global climatological  
466 dataset for drought forecasting. We strongly believe that the LSTM model has the forecasting capability  
467 to forecast droughts across different dataset type and drought indices, subsequent studies would be  
468 conducted to assert the findings. The findings from the study are as follows:

- 469 • The performance metrics for both SPEI 1 and SPEI 3 depicted excellent results highlighting its  
470 significance over other models. The  $R^2$  value for SPEI 1 and SPEI 3 achieved values of and 0.998  
471 and 0.996 respectively.
- 472 • However, the statistical metrics may not always reflect the variation and therefore a spatial  
473 analysis for the summer of 2017 and 2018 was conducted to examine how the index values vary  
474 at pixel level and across the summer seasons.
- 475 • The micro average value of ROC-AUC curves depicted value of 0.83 and 0.82 for SPEI 1 and  
476 SPEI 3 case, respectively. This could be a reflective of the threshold levels of drought categories,  
477 as few months depicted index values at the borderline. However, more stacked deep neural  
478 networks model would be built in the future, to improve our findings, especially for pixels  
479 representing values at the threshold point.

480 The applicability of the LSTM architecture needs to be tested in different climatic conditions to examine  
481 how well it captures the interrelationship between variables and drought index. The future works would  
482 also look towards involving climatic variables to forecast at longer time scales using deep learning  
483 techniques. It's well accepted that the use of deep neural networks would provide better forecasting  
484 results (Reichstein et al. 2019), the important aspect would be to interpret the model and provide a  
485 more in-depth explanation of the results (Dikshit et al. 2020c). The results from this study are useful  
486 for drought mitigation purposes, bushfires and for policy makers. The future study would look towards  
487 improving the LSTM architecture and use of different drought indices at both short-term and long-term  
488 drought scales, which would further enhance our understanding.

## 489 **Funding**

490 This research is funded by the Centre for Advanced Modelling and Geospatial Information Systems  
491 (CAMGIS), Faculty of engineering and IT, University of Technology Sydney.

## 492 **References**

- 493 1) ABARES (2016) Land Use of Australia 2010–11, ABARES, Canberra, May.
- 494 2) ABS (2018) Regional population by Age and Sex, Australia, 2017, cat. no. 3235.0 Australian  
495 Bureau of Statistics, Canberra
- 496 3) Alizadeh, M.R., Nikoo, M.R. (2018) A fusion-based methodology for meteorological drought  
497 estimation using remote sensing data. *Remote Sens. Environ.*, 211, 229-247.
- 498 4) Beard, G., E. Chandler, A. B. Watkins, and D. A. Jones (2011), How does the 2010- 11 La Niña  
499 compare with past La Niña events?, *Bull. Austral. Meteorol. Oceanogr. Soc.* 24, 17–20.



- 500 5) Beguería, S., Vicente-Serrano, S.M., Reig, F., Latorre, B. (2014) Standardized precipitation  
501 evapotranspiration index (SPEI) revisited: parameter fitting, evapotranspiration models, tools,  
502 datasets and drought monitoring. *International J of Climatology*, 34(10), 3001-3023
- 503 6) Bengio, Y., Simard, P., Frasconi, P. (1994) Learning long-term dependencies with gradient  
504 descent is difficult. *IEEE Trans. Neural Netw.*, 5, 157-166
- 505 7) Buda, M., Maki, A., Mazurowski, M.A. (2018) A systematic study of the class imbalance problem  
506 in convolutional neural networks. *Neural Networks*, 106, 249-259
- 507 8) Cai, W., Purich, A., Cowan, T. et al. (2014) Did climate change-induced rainfall trends  
508 contribute to the Australian Millennium Drought? *Journal of Climate*, 27, 3145-316
- 509 9) Dey, R., Lewis, S.C., Arblaster, J.M., Abram, N.J. (2019) A review of past and projected changes  
510 in Australia's rainfall. *Wiley Interdisciplinary Reviews: Climate Change*, 10, e577
- 511 10) Deo, R.C., Şahin, M. (2015) Application of the artificial neural network model for prediction of  
512 monthly standardized precipitation and evapotranspiration index using hydrometeorological  
513 parameters and climate indices in eastern Australia. *Atmos. Res.*, 161, 65–81
- 514 11) Deo, R.C., Kisi, O., Singh, V.P. (2017a) Drought forecasting in eastern Australia using  
515 multivariate adaptive regression spline, least square support vector machine and M5Tree  
516 model. *Atmos. Res.*, 184, 149-175
- 517 12) Deo, R.C., Tiwari, M.K., Adamowski, J.F., Quilty, J.M. (2017b) Forecasting effective drought  
518 index using a wavelet extreme learning machine (W-ELM) model. *Stoch Environ Res Risk  
519 Assess* 31:1211–1240
- 520 13) Dikshit, A., Pradhan, B., Alamri, A.M. (2020a) Temporal Hydrological Drought Index  
521 Forecasting for New South Wales, Australia using Machine Learning Approaches. *Atmosphere*,  
522 11(6), 585
- 523 14) Dikshit, A., Pradhan, B., Alamri, A.M. (2020b) Short-Term Spatio-Temporal Drought  
524 Forecasting Using Random Forests Model at New South Wales, Australia. *Appl. Sci.*, 10, 4254.
- 525 15) Dikshit, A., Pradhan, B., Alamri, A.M. (2020c) Pathways and challenges of the application of  
526 artificial intelligence to geohazards modelling. *Gondwana Res.*,  
527 <https://doi.org/10.1016/j.gr.2020.08.007>
- 528 16) Collobert, R., et al. (2011) Natural language processing (almost) from scratch. *J. Mach. Learn.  
529 Res.* 12, 2493–2537.
- 530 17) Farabet, C., Couprie, C., Najman, L., LeCun, Y. (2012) Scene parsing with multiscale feature  
531 learning, purity trees, and optimal covers. In *Proc. International Conference on Machine  
532 Learning* <http://arxiv.org/abs/1202.2160>
- 533 18) Francois, C. (2015) Keras. Github, <https://github.com/keras-team/keras>
- 534 19) Fung, K.F., Huang, Y.F., Koo, C.H., Soh, Y.W. (2019) Drought forecasting: A review of  
535 modelling approaches 2007–2017. *J. Water Clim. Chang.*
- 536 20) Goodfellow, I., Bengio, Y., Courville, A. (2016) Deep learning.
- 537 21) Ham, Y., Kim, J., Luo, J. (2019) Deep learning for multi-year ENSO forecasts. *Nature*, 573,  
538 568–572
- 539 22) Hao, Z., Singh, V.P. (2015) Drought characterization from a multivariate perspective: A review.  
540 *Journal of Hydrology*, 527, 668-678

- 541 23) Hao, Z., Hao, F., Xia, Y. et al. (2016) A Statistical Method for Categorical Drought Prediction  
542 Based on NLDAS-2. *J. Appl. Meteor. Climatol.*, 55 (4), 1049–1061.
- 543 24) Hao, Z., Singh, V.P., Xia, Y. (2018) Seasonal Drought Prediction: Advances, Challenges, and  
544 Future Prospects. *Reviews of Geophysics*. 56(1), 108-141
- 545 25) Harris, I. C. (2019) CRU TS v4.03: Climatic Research Unit (CRU) Time-Series (TS) version 4.03  
546 of high-resolution gridded data of month-by-month variation in climate (Jan. 1901- Dec. 2018).  
547 Centre for Environmental Data Analysis (CEDA),  
548 <https://doi.org/10.5285/10d3e3640f004c578403419aac167d82>
- 549 26) Harris, I., Osborn, T.J., Jones, P., Lister, D. (2020) Version 4 of the CRU TS monthly high-  
550 resolution gridded multivariate climate dataset. *Scientific Data*, 7, 109
- 551 27) Hayes, M., Svoboda, M., Wall, N., Widhalm, M. (2011) The Lincoln declaration on drought  
552 indices: universal meteorological drought index recommended. *Bulletin of the American*  
553 *Meteorological Society*, 92, 485-488.
- 554 28) Heberger, M. (2012) Australia's millennium drought: Impacts and responses. In *The world's*  
555 *water*, Springer, 97-125.
- 556 29) Hinton, G.E., Deng, L., Yu, D. et al. (2012) Deep neural networks for acoustic modeling in  
557 speech recognition: the shared views of four research groups. *IEEE Signal Processing Magazine*.  
558 29(6), 82-97
- 559 30) Hochreiter, S., Schmidhuber, J. (1997) Long short-term memory. *Neural Comput.*, 9, 1735-1780
- 560 31) Huete, A.R. (1988) A soil-adjusted vegetation index (SAVI). *Remote Sensing of Environment*,  
561 25(3), 295-309
- 562 32) Huntington, T. (2006), Evidence for intensification of the global water cycle: Review and  
563 synthesis, *J. Hydrol.*, 319(1–4), 83–95.
- 564 33) Krizhevsky, A., Sutskever, I., Hinton, G. (2012) ImageNet classification with deep convolutional  
565 neural networks. In *Proc. Advances in Neural Information Processing Systems 25* 1090–1098.
- 566 34) LeCun, Y., Bengio, Y., Hinton, G. (2015) Deep learning. *Nature* 521, 436–444
- 567 35) McKee, T.B., Doesken, N.J., Kleist, J. (1993) The relationship of drought frequency and  
568 duration to time scales. In *Proceedings of Proceedings of the 8th Conference on Applied*  
569 *Climatology*; pp. 179-183.
- 570 36) Mishra, A.K., Singh, V.P. (2010) A review of drought concepts. *Journal of hydrology*, 391, 202-  
571 216.
- 572 37) Mishra, A.K., Singh, V.P. (2011) Drought modeling–A review. *Journal of Hydrology*, 403, 157-  
573 175.
- 574 38) Mokhtarzad, M., Eskandari, F., Vanjani, N.J., Arabasadi, A. (2017) Drought forecasting by  
575 ANN, ANFIS, and SVM and comparison of the models. *Environ Earth Sci* 76, 729
- 576 39) Nagavciuc, V., Ionita, M., Perşoiu, A. et al. (2019) Stable oxygen isotopes in Romanian oak  
577 tree rings record summer droughts and associated large-scale circulation patterns over Europe.  
578 *Climate dynamics*, 52, 6557-6568.
- 579 40) Nolan, R.H., Boer, M.M., Collins, L. et al. (2020) Causes and consequences of eastern  
580 Australia's 2019- 20 season of mega- fires. *Global Change Biology*, 26(3):1039-1041

- 581 41) Olah, C. (2015) Understanding LSTM Networks, [http://colah.github.io/posts/2015-08-](http://colah.github.io/posts/2015-08-Understanding-LSTMs/)  
582 [Understanding-LSTMs/](http://colah.github.io/posts/2015-08-Understanding-LSTMs/)
- 583 42) Pedregosa F., Varoquaux G., Gramfort A., Michel V., Thirion B., Grisel O., et al. (2011) Scikit-  
584 learn: machine learning in python. *Journal of Machine Learning Research*, 12, 2825-2830
- 585 43) Pittock J, Grafton RQ and Williams J (2015) The MurrayDarling Basin Plan fails to deal  
586 adequately with climate change. *Water. Journal of the Australian Water Association*, 42(6): 28-  
587 34
- 588 44) Poornima, S., Pushpalatha, M. (2019) Drought prediction based on SPI and SPEI with varying  
589 timescales using LSTM recurrent neural network. *Soft Comput* 23, 8399–8412
- 590 45) Provost F., Domingos P. (2003) Tree induction for probability-based ranking. *Machine*  
591 *Learning*, 52 (3), 199-215
- 592 46) Reichstein, M., Camps-Valls, G., Stevens, B. et al. (2019) Deep learning and process  
593 understanding for data-driven Earth system science. *Nature* 566, 195–204
- 594 47) Renard, D., Tilman, D. (2019) National food production stabilized by crop diversity. *Nature*,  
595 571, 257-26
- 596 48) Rhee, J., Im, J. (2017) Meteorological drought forecasting for ungauged areas based on machine  
597 learning: Using long-range climate forecast and remote sensing data. *Agricultural and Forest*  
598 *Meteorology*, 237-238, 105-112
- 599 49) Schmidhuber, J. (2015) Deep learning in neural networks: An overview. *Neural Networks*, 61,  
600 85-117
- 601 50) Shen, R., Huang, A., Li, B., Guo, J. (2019) Construction of a drought monitoring model using  
602 deep learning based on multi-source remote sensing data. *International Journal of Applied*  
603 *Earth Observation and Geoinformation*, 79, 48-57
- 604 51) Silver, D. et al. (2016) Mastering the game of Go with deep neural networks and tree search.  
605 *Nature* 529, 484–489
- 606 52) Slette, I.J., Post, A.K., Awad, M et al. (2019) How ecologists define drought, and why we should  
607 do better. *Global Change Biology*, 25(10), 3193-3200
- 608 53) Spinoni, J., Barbosa, P., De Jager, A. et al. (2019) A new global database of meteorological  
609 drought events from 1951 to 2016. *J. Hydrol.-Reg. Stud.*, 22, 100593
- 610 54) Steffen, W., Hughes, L., Mulling, G., et al. (2019) Dangerous Summer: Escalating Bushfire, Heat  
611 and Drought Risk. Available: [https://www.climatecouncil.org.au/wp-](https://www.climatecouncil.org.au/wp-content/uploads/2019/12/report-dangerous-summer_V5.pdf)  
612 [content/uploads/2019/12/report-dangerous-summer\\_V5.pdf](https://www.climatecouncil.org.au/wp-content/uploads/2019/12/report-dangerous-summer_V5.pdf)
- 613 55) Sun, Q., Miao, C., Duan, Q. et al. (2018) A Review of Global Precipitation Data Sets: Data  
614 Sources, Estimation, and Intercomparisons. *Reviews of Geophysics*, 56(1):79-107
- 615 56) Van Asch, V. (2013) Macro-and micro-averaged evaluation measures [[basic draft]]. Belgium:  
616 CLiPS, 49.
- 617 57) Van Dijk, A.I.; Beck, H.E.; Crosbie, R.S. et al. (2013) The millennium drought in southeast  
618 Australia (2001–2009): Natural and human causes and implications for water resources,  
619 ecosystems, economy, and society. *Water Resour. Res.*, 49, 1040–1057.
- 620 58) Van Loon, A.F., Gleeson, T., Clark, J. et al. (2016) Drought in the Anthropocene. *Nature*  
621 *Geoscience*, 9, 89.

- 622 59) Vicente-Serrano, S.M., Beguería, S., López-Moreno, J.I. (2010) A multiscale drought index  
623 sensitive to global warming: the standardized precipitation evapotranspiration index. *Journal*  
624 *of climate*, 23, 1696-1718.
- 625 60) Vicente-Serrano, S.M., Begueria, S., Lorenzo-Lacruz, J., et al. (2012) Performance of Drought  
626 Indices for Ecological, Agricultural, and Hydrological Applications. *Earth Interactions*, 16(10),  
627 1-27
- 628 61) Wang, D., Borthwick, A.G., He, H., Wang, Y. et al. (2018) A hybrid wavelet de-noising and Rank-  
629 Set Pair Analysis approach for forecasting hydro-meteorological time series. *Environmental*  
630 *Research*, 160, 269-281
- 631 62) Williams, R.J., Zipser, D. (1989) A learning algorithm for continually running fully recurrent  
632 neural networks. *Neural Comput.*, 1, 270-280
- 633 63) Wittwer, G. (2020) Estimating the Regional Economic Impacts of the 2017 to 2019 Drought on  
634 NSW and the Rest of Australia; Victoria University, Centre of Policy Studies/IMPACT Centre:  
635 2020.
- 636 64) West, H., Quinn, N., Horswell, M. (2020) Remote sensing for drought monitoring & impact  
637 assessment: Progress, past challenges and future opportunities. *Remote Sensing of*  
638 *Environment*, 232, 111291
- 639 65) Xiao, C., Chen, N., Hu, C. et al. (2019) Short and mid-term sea surface temperature prediction  
640 using time-series satellite data and LSTM-AdaBoost combination approach. *Remote Sensing of*  
641 *Environment*, 223, 111358
- 642 66) Yihdego, Y., Vaheddoost, B., Al-Weshah, R.A. (2019) Drought indices and indicators revisited.  
643 *Arab J Geosci* 12, 69